XIAOYAN HU[1*], YINGBIN LIU[1], LI YANG[2], XIAOCHEN HUANG[3]

MICROSTRUCTURE AND MECHANICAL PROPERTIES OF STAINLESS STEEL/ALUMINUM MULTILAYER COMPOSITES BY ONE-STEP EXPLOSIVE WELDING

The stainless steel/aluminum multilayer composites were prepared by one-step explosive welding using ammonium nitrate explosive with two different thicknesses. The microstructure and mechanical properties of the multilayer composites were examined. There is a thin metallurgical melting zone at each bonding interface, consisting mostly of iron and aluminum elements. However, the micro-crack appears in the second metallurgical bonding zone obtained using the explosive of 24 mm thickness. The micro-hardness values at the four bonding interfaces are higher than those of bulk 1060 aluminum and 304 stainless steel. The yield strength of the multilayer composites obtained in the two cases is higher than that of the original 304 stainless steel while the tensile strength is between those of the original 1060 aluminum and 304 stainless steel. Meanwhile, the tensile strength and yield strength of multilayer composites obtained by explosive welding with explosive of 20 mm thickness are relatively higher.

Keywords: multilayer composites; one-step explosive welding; bonding interface; micro-hardness; mechanical properties

1. Introduction

Steel-aluminum composites are increasingly used in automobiles, pressure vessels, shipbuilding, chemical industry, heat exchanger production, military industry and other industries [1,2]. They possess the best microstructure properties and mechanical of the participating metals. It is challenging to join steel and aluminum through fusion welding techniques because of the significant differences in chemical and physical properties [3]. Efforts have been made to join these alloys together via friction stir welding [4-6], cold roll bonding [7], laser beam welding [8], resistance spot welding [9,10], brazed-fusion welding [11,12], and magnetic pulse welding [13]. However, these methods are generally appropriate for small welding samples of limited dimensions.

Explosive welding is a solid-phase welding process that combines two materials via a high-speed oblique collision powered by the explosive [14,15]. It is considered as an alternative method for welding aluminum and steel because it can weld larger-size samples and avoid excessive melting [14,16]. The welding of steel-aluminum by explosive welding has been reported [17-26]. However, the range of weldability between stainless steel and aluminum is restricted at a great level due to the large difference in their thermal conductivity [27]. Some scholars improved the welding quality of stainless steel-aluminum composites by reducing the explosion rate, adding an intermediate layer, using grooved substrate [22] and heat treatment [28,29]. Stainless steel [30], pure aluminum [18], copper [14], carbon steel [19], niobium [19], titanium [14], and tantalum [14] are often used as an intermediate layer in welding stainless steel and aluminum. The experimental results showed that the combination of interlayer and low-speed velocity explosive is an effective method for preparing stainless steel-aluminum composites with good performance [20].

Nowadays, multilayer metal composites are a progressive replacement for ordinary metal plates. The ideal quality of multilayer metal composites including alternative metal layers has been taken into consideration. The possibility of creating new properties by combining two or more metals in multilayered metal composites is a promising research direction in metal matrix composites [31]. Stainless steel/ aluminum multilayer has unique properties because of its favorable mechanical and thermal properties, and also of anti-corrosion characteristic of stainless steel, and electrical and thermal conductivity of aluminum. This composites are widely used in the decoration industry and household with various advantages.

[1] NORTH UNIVERSITY OF CHINA, SCHOOL OF ENVIRONMENT AND SAFETY ENGINEERING, TAIYUAN 030051, CHINA
[2] MILITARY PRODUCTS RESEARCH INSTITUTE, SHANXI JIANGYANG CHEMICAL CO., LTD., TAIYUAN 030051, CHINA
[3] CAPITAL AEROSPACE MACHINERY CORPORATION LIMITED, BEIJING 100076, CHINA

* Corresponding author: huxy85@nuc.edu.cn

Studies on stainless steel-aluminum explosive welding focused mainly on two-layer composites, while the explosive welding of stainless steel-aluminum multilayer composites was not reported.

This study attempts to produce a new five-layer stainless steel/ aluminum composites by one-step explosive welding method. The investigation of the microstructure and mechanical properties of the multilayer composites by this method can be effectively used in system design of new materials, and the prediction of the favorable properties of the multilayer composites.

2. Experimental procedure

304 stainless steels and 1060 aluminum with a thickness of 0.5 mm were used as raw materials. The thin-layer stainless steel/aluminum composites prepared by one-step explosive welding. The chemical compositions of the 304 stainless steel and 1060 aluminum are presented in TABLE 1 and TABLE 2, with hardness of 210 and 30 HV, respectively. The two aluminums were inserted into three stainless steels, maintaining a distance of 1 mm between the stainless steel layer and the aluminum layer, as shown in Fig. 1. The size of the plates was 60 mm × 200 mm × 0.5 mm. Two ammonium nitrate explosives with density of 0.8 g/cm^3, thickness of 20 mm and 24 mm, and detonation velocity of 2500 m/s were selected as the explosive welding explosives. The uppe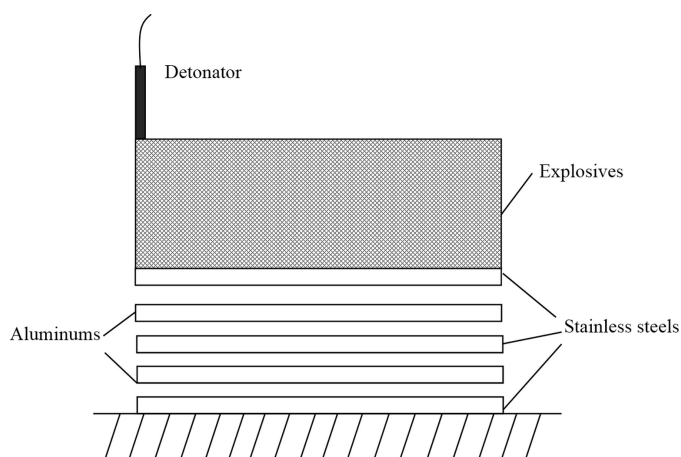r stainless steel served as the impact plate, and the explosive was directly placed on the upper stainless steel for explosive welding. The 8# electric detonator was used to detonate the explosive on the stainless steel. The kinetic energy of the detonation wave as well as explosion products was transferred to the stainless steel. The stainless steel moved downward at a certain speed and collided with other plates. Then, the explosive welding interface undergoes plastic deformation, local metal melting and atomic inter-diffusion, and finally a metal bond is formed [32].

In order to observe the interface bonding between the layers of the multilayer composites after explosive welding, the sample of 5 mm × 8 mm was taken out along the direction of detonation wave propagation on the multilayer composites using wire cutting device. The samples were respectively ground using water sandpaper of 600CW, 800CW, 1200CW, 2000CW and 2500CW in sequence. Finally, the samples were polished with alumina polishing paste with a particle size of 1 μm. The interface morphology and element distribution of stainless steel/aluminum multilayer composites were characterized by scanning electron microscopy (SEM) and energy dispersive X-ray energy spectrum (EDS). The mechanical properties such as micro-hardness, tensile strength and yield strength of stainless steel/aluminum multilayer composites were tested and analyzed.

The Vickers micro-hardness of the polished sample was measured using Shimadzu FM-300 micro-hardness tester. According to "GBT4340.1-2009 Vickers Hardness Test of Metallic Materials Part 1: Test Method", the test parameters are as follows: loading load was 200gf, pressing speed was 25 μm/s, loading time was 15s, and brightness was 60%.

The tensile test was carried out according to GB/T228-2010 "Metallic Materials Tensile Test Method at Room Temperature". The sample size was shown in Fig. 2, and the loading rate was 2 mm/min.
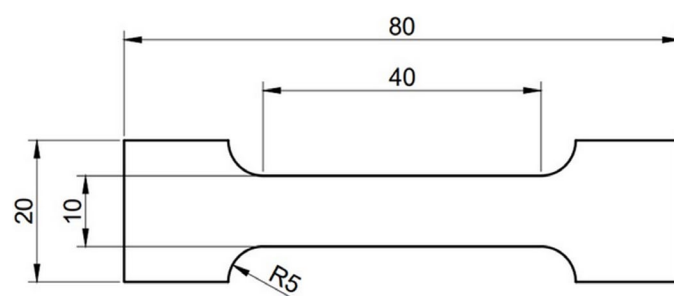

Fig. 1. Schematic diagram of explosive welding experimental device

Fig. 2. Tensile sample size

TABLE 1

Chemical composition of 304 stainless steel (wt%)

Element	C	Si	Mn	Ni	Cr	S	P	N	Fe
Content	≤0.08	≤1.00	≤2.00	8-15	18-20	≤0.03	≤0.035	≤0.1	Bal.

TABLE 2

Chemical composition of 1060 aluminum (wt%)

Element	Si	Fe	Cu	Mn	Mg	Zn	Ti	V	Al
Content	≤0.25	≤0.35	≤0.05	≤0.03	≤0.03	≤0.05	≤0.03	≤0.05	99.6

3. Results and discussion

3.1. Microstructural observation

Figs. 3 and Figs. 4 show the interface morphologies of the overall structure of the stainless steel/aluminum/stainless steel/aluminum/stainless steel multilayer composites explosive welded using two explosives with different thicknesses. To facilitate the interface that closest to the explosive downwards is called the first bonding interface, then, subsequently called the second bonding interface, the third bonding interface, and the fourth bonding interface. As seen, the bonding qualities between the layers of the multilayer composites obtained in both cases are good, that have no cracks, pores, or unbonding zones can be observed at the bonding interface of each layer. This result is consistent with that of two-layer stainless steel-aluminum composites by explosive welding [33,34]. This kind of bonding increases the bonding strength and related mechanical properties of composites to a certain extent [15]. Generally, the shape of the bonding interface of explosive welding composites is related to the explosive ratio and the properties of the welded materials [33,35-38]. In both cases, the widths of the metallurgical melt-

ing layer at the second bonding interface and the fourth bonding interface are wider than those at the first bonding interface and the third bonding interface, respectively.

Since the explosive welding process takes place in a very short period of time, the lower plate could not respond at the moment of plate-plate collision. Assuming that the collision velocities of the first layer are the same everywhere and are expressed by v_1, the mass of the plate per unit area is expressed by m_{1i}, and the mass per unit area of the second plate that collides with the first layer is expressed by m_{2i}, then the common velocity of the two plates after collision is v_2. Therefore, according to the law of momentum conservation:

$$m_{1i}v_1 = (m_{1i} + m_{2i})v_2 \tag{1}$$

$$\sum m_{1i}v_1 = \sum (m_{1i} + m_{2i})v_2 \tag{2}$$

Then, the energy lost after the collision between the first layer and the second layer, that is, the energy absorbed ΔE_1 by the deformation and interface bonding of the two layers is:

$$\Delta E_1 = \frac{1}{2}m_1v_1^2 - \frac{1}{2}(m_1 + m_2)v_2^2 = \frac{1}{2}\frac{m_1m_2}{m_1 + m_2}v_1^2 \tag{3}$$
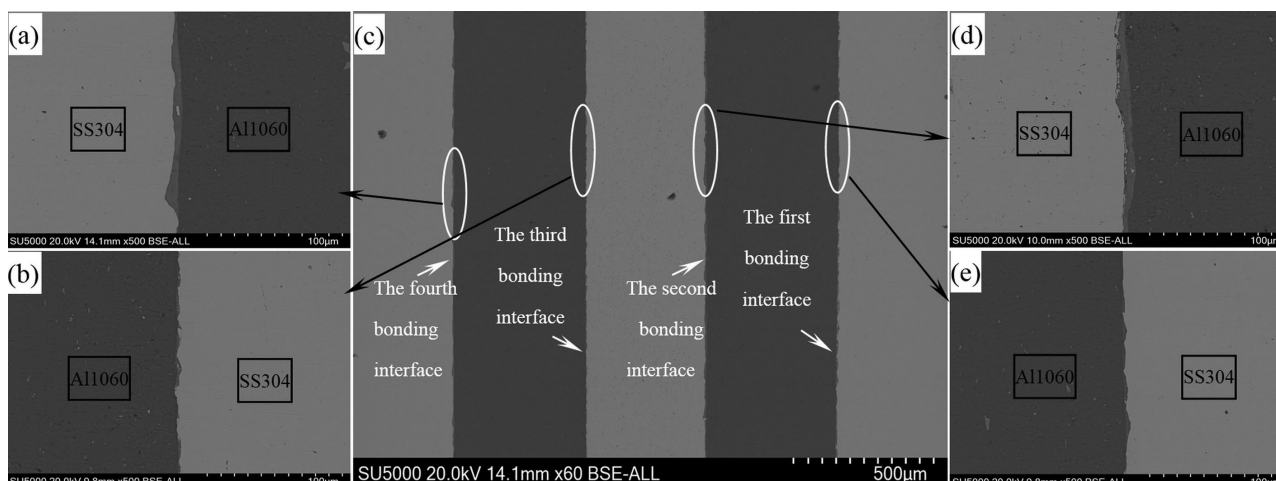

Fig. 3. The interface morphologies of the multilayer composites explosive welded with explosive of 20 mm thickness
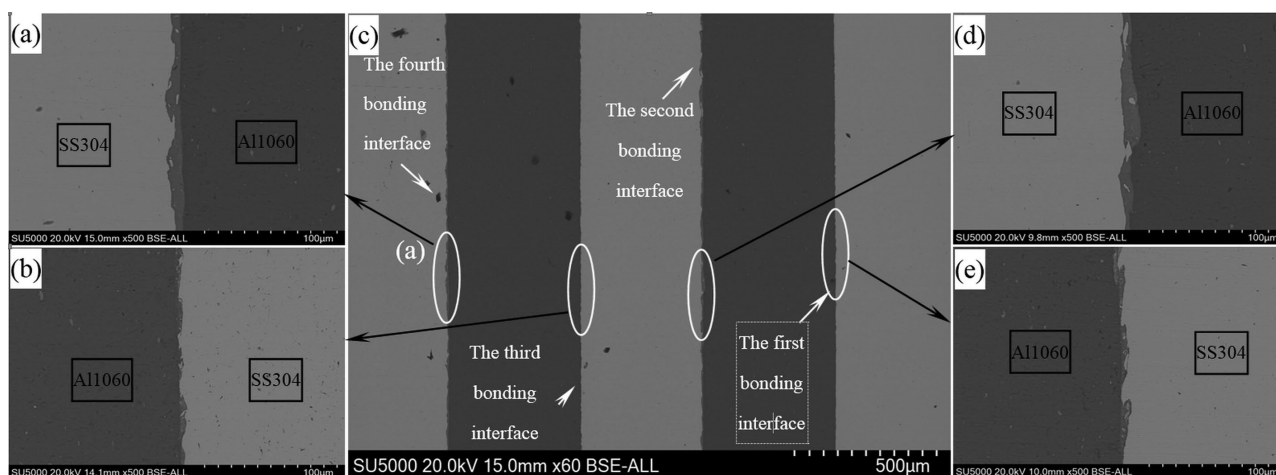

Fig. 4. The interface morphologies of the multilayer composites explosive welded with explosive of 24 mm thickness
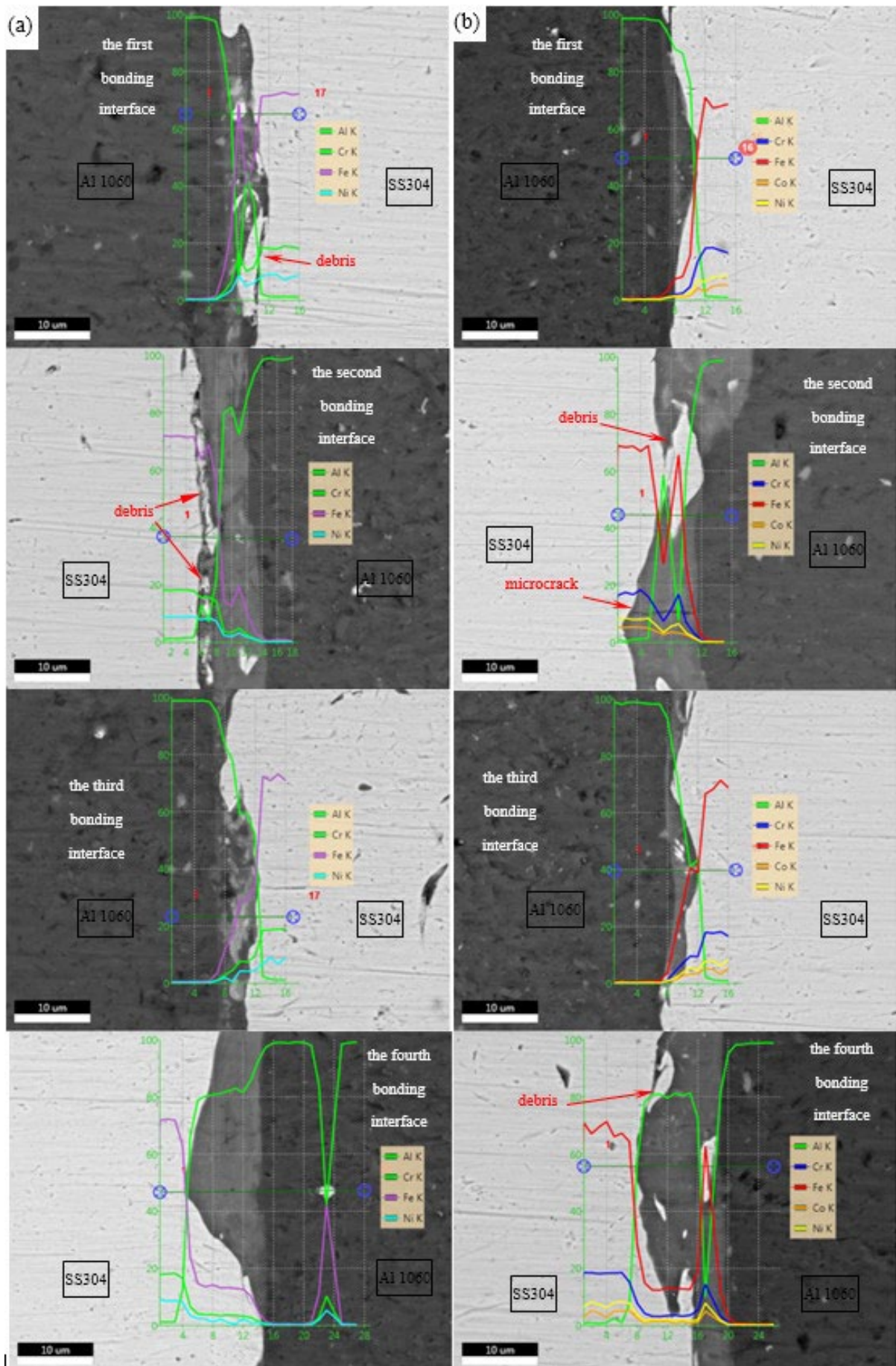
942

Fig. 5. The element distribution at each bonding interface of the multilayer composites explosive welded using two explosives with different thicknesses: (a) 20 mm and (b) 24 mm

According to reference [39], the quality of the bonding interface of explosive welding composites depends on the control of dynamic mechanical parameters. The main dynamic mechanical parameters of explosive welding include the impact angle θ, the moving velocity of the collision point v_c and the collision velocity v_p, and the relationship among the three is shown as follows [40].

$$v_p = 2v_c \sin \frac{\theta}{2} \qquad (4)$$

These parameters are related to the explosive velocity and explosive ratio. For parallel explosive welding, the moving velocity of the collision point is equal to the explosive detonation velocity, and the collision velocity can be calculated by the following formula [41,42]:

$$v_p = \sqrt{2E \frac{3R^2}{R^2 + 5R + 4}} \qquad (5)$$

$$E = \frac{1}{\gamma^2 - 1} \left(\frac{\gamma}{\gamma + 1} \right)^{\gamma} v_d^2 \qquad (6)$$

$$R = \frac{\rho_0 t_0}{\rho_1 t_1} \qquad (7)$$

Where, E is the Gurney energy of the explosive. R is the mass ratio of the explosive per unit area to the flyer plate. v_d is the explosive detonation velocity. γ is the polytropic exponent of explosive, and the value for ammonium nitrate explosive is 2. ρ_0 and ρ_1 are the density of explosive and flyer plate. t_0 and t_1 are the thickness of explosive and flyer plate per unit area.

Consequently, the relevant dynamic parameters when the first layer and the second layer collide and the energy lost after the collision can be calculated, as shown in TABLE 3.

TABLE 3

Dynamic parameters for explosive welding

Explosive thickness (mm)	R	v_c (m/s)	v_p (m/s)	v_2 (m/s)	v_3 (m/s)	v_4 (m/s)
20	4.04	2500	1495.9	1118.0	639.8	559.0
24	4.84	2500	1587.7	1186.7	679.1	593.3

The calculations show that some of the energy is lost after the collision between the first layer and the second layer. That is, the collision speed was low when the first and second layers collided with the third layer. However, the width of the metallurgical melting bonding at the second bonding interface is wider than that at the first bonding interface, which indicates that the material properties of the flyer affect the quality of the bonding interface. This result is identical to that in reference [43].

Fig. 5 shows the element distribution at each bonding interface respectively. As seen, mutual diffusion between elements appears at the four bonding interfaces, indicating that they are composed of intermetallic compounds and metallurgical melting

bonding is formed at the interfaces [44,45]. At the same time, the distribution of atoms at each bonding interface is unstable. This indicates that the metallurgical melt layer is likely to be composed of unstable compounds. Granulated debris appears in the melting area close to the steel at the interfaces. In the explosive welding process, tremendous energy was generated due to the high-speed collision between the plates, making the stainless steel at the bonding interface crumble. Crushed stainless steel cools rapidly and then forms a micro volume with weak constraints [45]. Furthermore, micro-crack appears in the second bonding interface obtained using the explosive with 24 mm thickness (Fig. 5), which has some limitations on the further application of explosive welded composites. This phenomenon shows that the explosive energy with 24 mm thickness was too high for explosive welding of five-layer stainless steel/aluminum. In explosive welding, the wavy interface of composites is more suitable, which makes the composites have better mechanical properties. But in multilayer explosive welding, too little energy will result in the failure of bonding interface away from explosive.

3.2. Micro-hardness

The micro-hardness measurement indicates that the micro-hardness performance of every aluminum and stainless steel after explosive welding is better than those of the raw materials respectively (Fig. 6). The micro-hardness values of the four bonding interfaces are higher than those of bulk aluminum and bulk stainless steel. It is mainly because of the severe plastic deformations at the bonding interface and the formation of thin metallurgical melting. This phenomenon is consistent with the two-layer steel-aluminum explosive welding [46]. Meanwhile, different degrees of plastic deformation also occured at the metals away from the bonding interfaces during the explosive welding process. These deformations can increase the micro-hardness
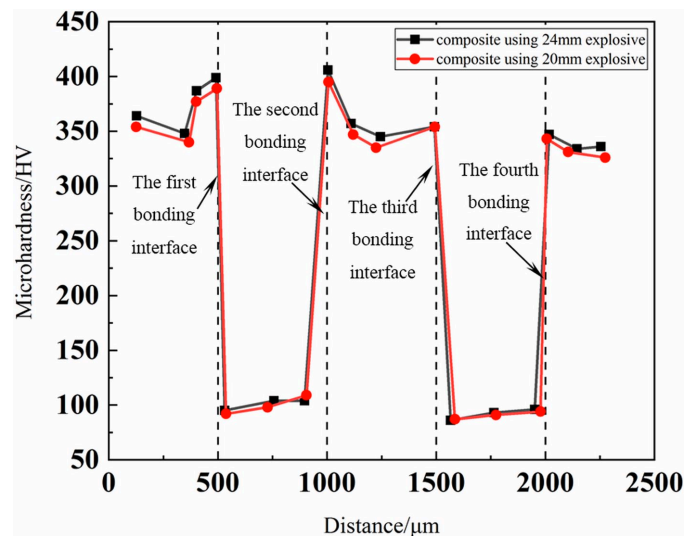

Fig. 6. The micro-hardness distribution in the multilayer composites explosive welded using two explosives with different thicknesses

944

of the corresponding area. As the distance from the bonding interface increases, the degree of plastic deformation decreases. As a result, the micro-hardness values of the bonding interfaces are much higher. Furthermore, from the first bonding interface to the fourth bonding interface, the collision velocity varies from high to low. As a result, the further away from the explosive is, the lower the degree of plastic deformation at the bonding interface. By comparison, the micro-hardness value of the multilayer composites obtained with a thicker explosive at the same position is higher. During explosive welding, the energy of the explosive determines the collision speed between the plates. The higher the energy and the higher the collision speed would be, leading to the greater plastic deformation and hardening degree of the interface and the metal plate.

3.3. Mechanical properties

Fig. 7 shows the stress-strain curve of experimental materials and TABLE 4 shows the yield strength and tensile strength of the multilayer composites before and after explosive welding.
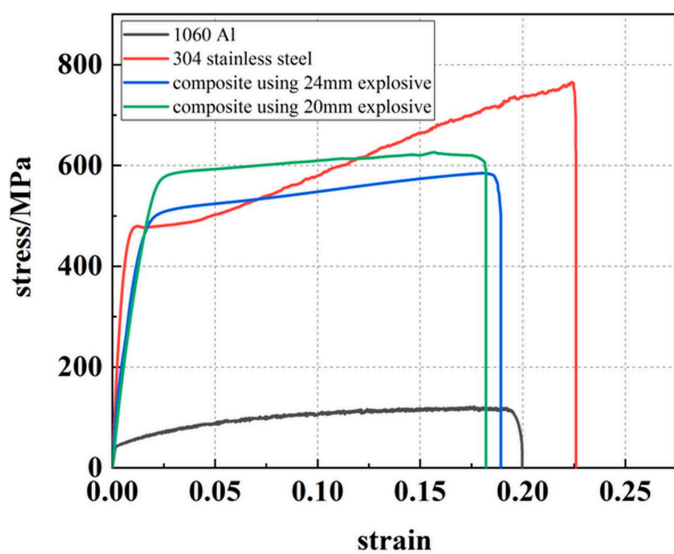

Fig. 7. The stress-strain curve of all experimental materials

TABLE 4

The results of tensile tests

	Yield Strength /MPa	Tensile Strength /MPa
1060 aluminum	42	118
304 stainless steel	478	765
Multilayer composite using 20 mm explosive	578	620
Multilayer composite using 24 mm explosive	502	585

It can be seen that the yield strength of the multilayer composites obtained in the two cases is higher than that of the original 304 stainless steel. The tensile strength of the multilayer

composites is between those of the original 1060 aluminum and 304 stainless steel. This is mainly because that during the collision, each layer of the plate has different forms and different degrees of plastic deformation and organizational changes, increasing the deformation resistance of multilayer composites significantly. These deformations not only could increase the micro-hardness at the corresponding position but also enhance the strength of the multilayer composites. In addition, the multilayer composites combine the high deformation resistance of stainless steel with the excellent plasticity and toughness of aluminum. Comparing the mechanical properties of composites under the two conditions, it is found that the tensile strength and yield strength of multilayer composites obtained using the explosive with 20 mm thickness were relatively higher. In the explosive welding process, the microscopic defects appeared in multilayer composites obtained using the explosive with 24mm thickness due to excessive energy. The tensile fracture morphology of the bonding interfaces of the multilayer composites obtained by explosive welding with explosive of 20 mm thickness is shown in Fig. 8. It is observed that there is no obvious separation at the bonding interfaces, means the excellent quality of interface bonding. The matrix aluminum layer and stainless steel layer show an obvious ductile fracture. However, the stainless steel near the interface has micro-zone brittle fracture. In the process of explosive welding, the unstable energy of detonation wave leads to the embrittlement of some stainless steels.
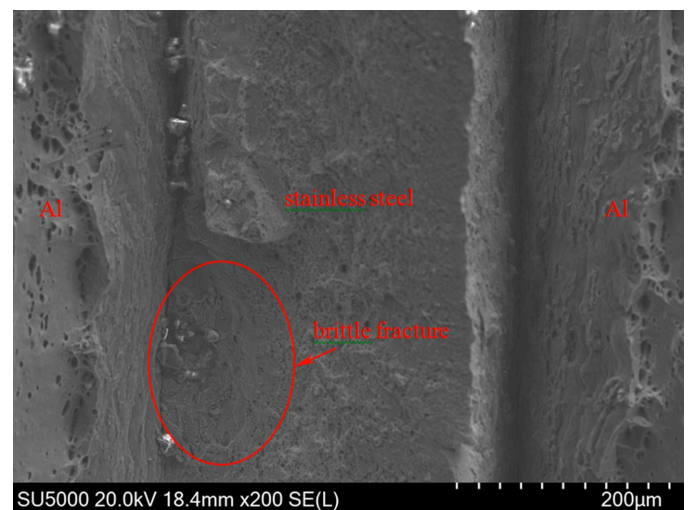

Fig. 8. The tensile fracture morphology of the multilayer composites obtained by explosive welding with explosive of 20 mm thickness

4. Conclusions

In this study, the interfacial bonding quality and mechanical properties of stainless steel/aluminum multilayer composites prepared by one-step explosive welding using ammonium nitrate explosives of 20 mm and 24 mm thicknesses were researched respectively. The following conclusions can be drawn from this study:

In both cases, the thin metallurgical melting layers are found on the four bonding interfaces of the multilayer composites. And the widths of the metallurgical melting layer at the second bonding interface and the fourth bonding interface are wider than those at the first bonding interface and the third bonding interface, respectively. However, the micro-crack appears at the second metallurgical bonding zone of the multilayer composites using explosive of 24 mm thickness.

The micro-hardness values at the four bonding interfaces are higher than those of bulk 1060 aluminum and 304 stainless steel. Meanwhile, the micro-hardness value of the multilayer composites obtained with thicker explosive at the same position is higher.

The yield strength of the multilayer composites obtained in the two cases is higher than that of the original 304 stainless steel while the tensile strength was between that of the original 1060 aluminum and 304 stainless steel. Meanwhile, the tensile strength and yield strength of multilayer composites obtained by explosive welding with explosive of 20 mm thickness are relatively higher.

The specific composition of the metallurgical melting layer has not been adequately analyzed. In addition, the microstructure and mechanical properties of multilayer composites with two kinds of explosive thickness were studied. The relevant experimental investigation under other loadings may provide a better understanding of the properties.

REFERENCES

[1] A. Gullino, P. Matteis, F. D'Aiuto, Metals-Basel **9**, 315 (2019).

[2] M.M. Atabaki, M. Nikodinovski, P. Chenier, J. Ma, M. Harooni, R. Kovacevic, Journal for Manufacturing Science and Production **14**, 59-78 (2014).

[3] R. Indhu, S. Soundarapandian and L. Vijayaraghavan, J. Mater. Process. Technol. **262**, 411-421 (2018).

[4] Z. Shen, Y. Ding, J. Chen, B.S. Amirkhiz, J.Z. Wen, L. Fu, A.P. Gerlich, Journal of Materials Science & Technology **35**, 1027-1038 (2019).

[5] P. Li, S. Chen, H.G. Dong, H. Ji, Y.B. Li, X. Guo, G.S. Yang, X.S. Zhang, X.L. Han, J. Manuf. Process. **49**, 385-396 (2020).

[6] H. Shan, Y.W. Ma, S.Z. Niu, B.X. Yang, M. Lou, Y.B. Li, Z.Q. Lin, J. Mater. Process. Tech. **295**, 117156 (2021).

[7] H.R. Akramifard, H. Mirzadeh, M.H. Parsa, Mat. Sci. Eng. A-Struct. **613**, 232-239 (2014).

[8] Y.L. Li, Y.R. Liu, J. Yang, Optics and Laser Technology **122**, 105875 (2020).

[9] W.H. Zhang, D.Q. Sun, L.J. Han, D.Y. Liu, Mater. Design **57**, 186-194 (2014).

[10] S.Q. Hu, A.S. Haselhuhn, Y.W. Ma, Y.B. Li, B.E. Carlson, Z.Q. Lin, J. Manuf. Process. **68**, 534-545 (2021).

[11] G.L. Qin, Z.Y. Ao, Y. Chen, C.S. Zhang, P.H. Geng, J. Mater. Process. Tech. **273**, 116255 (2019).

[12] F. Yan, K. Zhang, B.Y. Yang, Z. Chen, Z.W. Zhu, C.M. Wang, Optics and Laser Technology **138**, 106834 (2021).

[13] H.P. Yu, H.Q. Dang, Y.N. Qiu, J. Mater. Process. Tech. **250**, 297-303 (2017).

[14] S.M. Aceves, F.Espinosa-Loza, J.W. Elmer, R. Huber, Int. J. Hydrogen Energy **40**, 1490-1503 (2015).

[15] F. Findik, Mater. Design **32**, 1081-1093 (2011).

[16] N. Becker, D. Gauthier, E.E. Vidal, International Journal of Fatigue **139**, 105736 (2020).

[17] X.J. Sun, J. Tao, X.Z. Guo, T. Nonferr. Metal. Soc. **21**, 2175-2180 (2011).

[18] G.H.S.F.L. Carvalho, I. Galvao, R. Mendes, R.M. Leal, A. Loureiro, Mater. Charact. **155**, 109819 (2019).

[19] G.H.S.F.L. Carvalho, I. Galvao, R. Mendes, R.M. Leal, A. Loureiro, J. Mater. Process. Tech. **283**, 116707 (2020).

[20] G.H.S.F.L. Carvalho, I. Galvao, R. Mendes, R.M. Leal, A. Loureiro, Metals-Basel **10**, 1062 (2020).

[21] Q. Chu, T. Xia, P. Zhao, M. Zhang, J. Zheng, F. Yan, P. Cheng, C. Yan, C. Liu, H. Luo, Mat. Sci. Eng. A-Struct. **833**, 142525 (2022).

[22] C.W.D. Kumar, S. Saravanan, K. Raghukandan, Transactions of the Indian Institute of Metals **72**, 3269-3276 (2019).

[23] X. Li, H. Ma, Z. Shen, Materials & Design **87**, 815-824 (2015).

[24] H. Pouraliakbar, G. Khalaj, M.R. Jandaghi, A. Fadaei, M.K.Ghareh-Shiran, S.H. Shim, S.I. Hong, International Journal of Pressure Vessels and Piping **188**, 104216 (2020).

[25] M. Yang, H.-H. Ma, Z.-W. Shen, D.-G. Chen, Y.-X. Deng, T. Nonferr. Metal. Soc. **29**, 680-691 (2019).

[26] Y.-L. Sun, H.-H. Ma, M. Yang, Z.-W. Shen, N. Luo, L.-Q. Wang, Coatings **10**, 1031 (2020).

[27] G.H.S.F.L. Carvalho, I. Galvao, R. Mendes, R.M. Leal, A. Loureiro, J. Mater. Process. Tech. **262**, 340-349 (2018).

[28] M.K.G. Shiran, S.J.M. Baygi, S.R. Kiahoseyni, H. Bakhtiari, M.A. Dadi, International Journal of Damage Mechanics **27**, 488-506 (2018).

[29] M.K.G. Shiran, G. Khalaj, H. Pouraliakbar, M. Jandaghi, H. Bakhtiari, M. Shirazi, Int. J. Min. Met. Mater. **24**, 1267-1277 (2017).

[30] T. Izuma, K. Hokamoto, M. Fujita, M. Aoyagi, Welding International **6**, 941-946 (1992).

[31] H. Mansouri, B. Eghbali, M. Afrand, J. Manuf. Process. **46**, 298-303 (2019).

[32] V.I. Lysak, S.V. Kuzmin, J. Mater. Process. Technol. **222**, 356-364 (2015).

[33] G.H.S.F.L. Carvalho, I. Galvao, R. Mendes, R.M. Leal, A. Loureiro, Mater. Charact. **142**, 432-442 (2018).

[34] X.-J. Sun, J. Tao, X.-Z. Guo, Transactions of Nonferrous Metals Society of China **21**, 2175-2180 (2011).

946

[35] M. Yang, H. Ma, Z. Shen, Y. Sun, Fusion Eng. Des. **143**, 106-114 (2019).

[36] G.H.S.F.L. Carvalho, I. Galvao, R. Mendes, R.M. Leal, A. Loureiro, Int. J. Adv. Manuf. Tech. **103**, 3211-3221 (2019).

[37] G.H.S.F.L. Carvalho, I. Galvao, R. Mendes, R.M. Leal, A. Loureiro, Sci. Technol. Weld. Joining **23**, 501-507 (2018).

[38] H.B. Xia, S.G. Wang, H.F. Ben, Materials & Design **56**, 1014-1019 (2014).

[39] M.H. Bina, F. Dehghani, M. Salimi, Mater. Design **45**, 504-509 (2013).

[40] Z. Zheng, Explosive working, National Defense Industry Press, Beijing (1981).

[41] M.M.H. Athar, B. Tolaminejad, Mater. Design **86**, 516-525 (2015).

[42] A. Koch, N. Arnold, M. Estermann, Propellants, Explosives, Pyrotechnics **27**, 365-368 (2002).

[43] G.H.S.F.L. Carvalho, I. Galvão, R. Mendes, R.M. Leal, A. Loureiro, J. Mater. Process. Tech. **262**, 340-349 (2018).

[44] M. Fan, W. Yu, W. Wang, X. Guo, K. Jin, R. Miao, W. Hou, N. Kim, J. Tao, J. Mater. Eng. Perform. **26**, 277-284 (2017).

[45] S.V. Gladkovsky, S.V. Kuteneva, S.N. Sergeev, Mater. Charact. **154**, 294-303 (2019).

[46] X. Guo, M. Fan, L. Wang, F. Ma, J. Mater. Eng. Perform. **25**, 2157-2163 (2016).